Journal of Microbiology, Immunology and Infection 56 (2023) 20—30

Available online at www.sciencedirect.com

ScienceDirect

journal homepage: www.e-jmii.com

Original Article

Interdependence of glycemic and lipid modulation in cured chronic hepatitis C patients by direct-acting antiviral agents

Pin-Nan Cheng [a,1], Hung-Yu Sun [b,c,d,1], I-Che Feng [e], Yen-Cheng Chiu [a], Sin-Tian Wang [f], Dyoness Charmaine Tan [f], Hung-Chih Chiu [a], Shih-Chih Chien [a], Kung-Chia Young [f,g,*]

[a] *Department of Internal Medicine, National Cheng Kung University Hospital, College of Medicine, National Cheng Kung University, Tainan, Taiwan*
[b] *Department of Biomedical Engineering, College of Biology, Hunan University, Changsha, China*
[c] *Institute of Pathogen Biology and Immunology of College of Biology, Hunan Provincial Key Laboratory of Medical Virology, Hunan University, Changsha, China*
[d] *Institute of Molecular Medicine, College of Medicine, National Cheng Kung University, Tainan, Taiwan*
[e] *Department of Internal Medicine, Chi-Mei Medical Center, Tainan, Taiwan*
[f] *Department of Medical Laboratory Science and Biotechnology, College of Medicine, National Cheng Kung University, Tainan, Taiwan*
[g] *Center of Infectious Disease and Signaling Research, College of Medicine, National Cheng Kung University, Tainan, Taiwan*

Received 6 November 2021; received in revised form 1 May 2022; accepted 16 June 2022
Available online 6 July 2022

KEYWORDS
Glycemic parameters;
Hepatitis C virus;
Lipid metabolism;
Post-therapy;
Sustained virological response

Abstract *Background:* Chronic hepatitis C virus (HCV) infection causes various liver diseases and metabolic disorders. With direct-acting antiviral agents (DAAs), which effectively eradicate pan-genotypic HCV, hepatic and concomitant metabolic restorations are achieved. The study aims to evaluate the posttherapeutic benefits of lipid and glycemic homeostasis.
Methods: Nighty-five chronic hepatitis C patients who achieved sustained virological response (SVR) by using DAAs were enrolled to collect plasma samples and fractionated lipoproteins at baseline, SVR, and during the post-SVR follow-ups for 6 months (pS6m) and 1 year (pS1yr). The lipid and glycemic parameters were analyzed to establish muturally modulatory relationships.
Results: Plasma cholesterol (Chol) and glucose were elevated at SVR from baseline, whereas plasma Chol remained increased until pS1yr; however, glucose returned to the basal level. The post-SVR responses included a peak elevation of glycated hemoglobin at pS6m, a sustained elevation of triglyceride (Tg), and sustained declines in insulin, homeostasis model assessment

* Corresponding author. Department of Medical Laboratory Science and Biotechnology, College of Medicine, National Cheng Kung University, No. 1 University Rd., Tainan, 70101, Taiwan. Fax: +886 6 2363956.
E-mail address: t7908077@mail.ncku.edu.tw (K.-C. Young).
[1] Equal contribution.

https://doi.org/10.1016/j.jmii.2022.06.004

(HOMA)-insulin resistance, and HOMA-beta levels until pS1yr. The changes in plasma Chol and high-density-lipoprotein Chol showed positive correlations, as did the plasma Tg with low-density-lipoprotein Tg and very-low-density-lipoprotein Tg *per* particle load. Very-low-density-lipoprotein was found to be loaded with increased Tg and Chol and underwent efficient Tg catabolism in the form of conversion into low-density-lipoprotein. Additionally, the post-therapeutic dynamics exhibited correlations of high-density-lipoprotein Chol with plasma glucose and HOMA-beta.

Conclusion: Irrespective of the baseline metabolic status, the posttherapeutic interdependent modulation of blood glycemic and lipid metabolic parameters were revealed in chronic hepatitis C patients following clearance of HCV viremia by DAA treatment.

Introduction

Hepatitis C virus (HCV) infection causes hepatic inflammation that may lead to end-stage liver diseases; additionally, it dysregulates systemic metabolic homeostasis in association with various metabolic disorders, such as insulin resistance (IR), type II diabetes, and cardiovascular diseases (CVDs).[1] Chronic hepatitis C (CHC) represents a considerable disease burden by affecting 71 million people worldwide.[2] Fortunately, the current direct-acting antiviral agents (DAAs) for the treatment of CHC can exert a highly efficient sustained virological response (SVR) and thus reducing liver-related outcomes,[3—6] accompanied by decreased cardiometabolic risks in limited study populations.[7,8] Nevertheless, more studies are required across geographic areas and ethnics to ensure the post-therapeutic benefits in CHC patients after achieving SVR.

The manner in which DAA treatment for CHC influences glucose-lipid metabolic dysfunction remains elusive. HCV infection disturbs host glycemic and lipid metabolism via molecular mechanisms that may partially impair insulin signaling pathways[6] by the direct viral components, such as the way of HCV core protein-mediated degradation of insulin receptor substrate 1 or 2, as well as indirectly by inducing oxidative stress and inflammatory cytokines, such as tumor necrosis factor alpha.[9,10] Glucose metabolism can be affected by HCV infection, which reduces glucose uptake and sustains gluconeogenesis in conjunction with hepatic insulin resistance (IR).[11,12] Furthermore, HCV depends on the host lipid metabolism in its lifecycle,[13] utilizes very-low-density lipoprotein (VLDL) biogenesis machinery to produce infectious viral particles,[14,15] and predisposes hepatocytes to lipid metabolism derangements that enhance lipogenesis[16]; however, reduce lipoprotein secretion and β-oxidation of lipids.[17] Taken together, the impairments of glycemic and lipid metabolism by HCV infection may be interdependently regulated.

CHC patients are prone to exhibit hyperglycemia, hypocholesterolemia, hypobeta-lipoproteinemia, and hypotriglyceridemia[18] as a result of host sugar and fat metabolic dysregulations, which have been associated with unsatisfactory outcomes of interferon-based therapy and severe liver disease progression.[19] The current highly efficient DAA treatment options have been able to exert >95% viral eradication of pangenotypic HCV in CHC patients, thus improving liver-related outcomes that are accompanied by the repair of metabolic dysfunction.[20—22] The question to be addressed was focused on the post-SVR sustained improvement of glycemic and lipid homeostasis, as well as the influence on CVD risks. In this study, the regulatory events and sequential associations between the metabolism parameters in circulation were evaluated at baseline, SVR (post end-of-treatment for 3 months), post-SVR for 6 months (pS6m), and post-SVR for 1 year (pS1yr).

Materials and methods

Patients

This study recruited 95 CHC patients (28 males and 67 females, with ages ranging from 40 to 87 years), of whom 59 and 36 patients had HCV genotypes 1 and 2, respectively. The baseline characteristics of the patients are shown in Suppl. Table 1. All of the patients achieved SVR after receiving the 12-week DAA treatments, as recommended, including paritaprevir/ritonavir-ombitasvir and dasabuvir (PrOD) ± ribavirin (RBV) (35/95), sofosbuvir/daclatasvir/ledipasvir ± ribavirin (RBV) (36/95), elbasvir/grazoprevir (12/95), and 8-week glecaprevir/pibrentasvir (2/95). None of the patients used lipid-lowering agents during the periods of treatment and follow-up. Plasma samples were collected with overnight fasting at baseline, SVR, pS6m, and pS1yr. All of the participants were enrolled from the National Cheng Kung University Hospital, with each participant signing an informed consent form, and the study was approved by the local Institutional Review Board.

Isolation of lipoprotein classes and quantification of Tg, Chol, and apoB

High-density lipoprotein (HDL) was separated from the non-HDL fraction with the phosphotungstic acid precipitation method (Fortress Diagnostics, UK). VLDL and low-density lipoprotein (LDL) particles were isolated by using iodixanol density-gradient ultracentrifugation, as has been previously described.[23] The peaks corresponding to VLDL (density of 1.0015—1.0050 g/ml) and LDL (density of 1.025—1.035 g/

Table 1 The correlations of the changes of Chol and Tg levels between in plasma and in individual HDL, VLDL, and LDL within the indicated time intervals.

Time intervals	Chol			Tg		
	VLDL	LDL	HDL	VLDL	LDL	HDL
Baseline to SVR (% of changes to baseline)	0.015 (0.927)	0.278 (0.091)	0.552 (<0.001)	0.070 (0.672)	0.596 (<0.001)	0.118 (0.385)
SVR to pS6m (% of changes to SVR)	0.121 (0.462)	0.082 (0.626)	0.277 (0.010)	0.003 (0.987)	0.034 (0.840)	0.219 (0.119)
pS6m to pS1yr (% of changes to pS6m)	0.076 (0.647)	0.278 (0.087)	0.138 (0.204)	0.406 (0.010)	0.421 (0.008)	0.035 (0.804)

Data were expressed as Pearson coefficient (*p* value).

ml) were separately collected after centrifugation at 95,000 rpm (MLA-130 rotor, Beckman) for 3 h at 16 °C.

Laboratory assessments

Biochemical parameters in plasma or serum samples were extracted from the automation routine laboratories of the NCKU Hospital. Homeostasis model assessment (HOMA)-insulin resistance (IR) and HOMA-beta values were also calculated.[24] HCV-RNA titers (RealTime HCV quantitative assay) and genotypes (RealTime HCV Genotype II assay) were determined by using the corresponding methods (Abbott Molecular, IL).

The Tg and Chol contents in each HDL, VLDL, and LDL fraction were quantified by the corresponding biochemical assay kits (Fortress Diagnostics, UK). The lipid values in plasma and HDLs were expressed by the units wt/vol, and those values in VLDL and LDL fractions were expressed by the units wt/wt, according to normalization with apoB, which was determined via the ELISA technique[23] by using capture anti-apoB (Millipore, USA), peroxidase-conjugated polyclonal goat anti-apoB, and BM Chemiluminescence substrate (Roche Diagnostics, USA). The VLDL particles are assembled with lipids and apoB in hepatocytes and exported into the bloodstream, where substantial amounts of Tg undergo hydrolysis until its conversion into LDL. Due to the fact that apoB maintains a one-to-one molar ratio from VLDL to LDL conversion, the lipid loading capacity *per* lipoprotein particle unit can be evaluated after normalization to apoB.[23]

Statistical analysis

The continuous variables and analytical data are described as the mean ± SEM. The differences between the groups were evaluated via the Mann-Whitney test, pair t-test, and Chi-square test, as appropriate. The dynamic changes in the analytical data were assessed by using one-way ANOVA with repeated measures adjusted for age, gender, and HCV genotype; additionally, changes between HCV genotypes 1 and 2 were analyzed via a linear mixed model analysis adjusted for age and gender. The associations between indicated parameters were analyzed by using Pearson's correlation analysis. All of the statistical analyses were conducted by using SPSS software (version 19.0; SPSS, Inc., Chicago, IL).

Results

The regulations of plasma glucose and Chol coincided at SVR

The pretreatment data of the CHC patients (n = 95), including those data for HCV genotype 1 (n = 59) and genotype 2 (n = 36), are summarized in Suppl. Table 1. The analytic results of the plasma samples at baseline, SVR, pS6m, and pS1yr were compared.

First, the glycemic and lipid responses in patients receiving DAA treatment were evaluated. When compared to baseline, plasma glucose (110.4 ± 3.2 *vs.* 104.7 ± 2.2 mg/dL, p = 0.012, Fig. 1A) and Chol levels (176.6 ± 3.1 *vs.* 156.7 ± 2.7 mg/dL, p < 0.001, Fig. 1B) at SVR were elevated. However, the post-SVR glucose levels returned to the baseline level at pS6m (Fig. 1A), whereas plasma Chol levels remained constantly high until pS1yr (Fig. 1B, p < 0.001).

The post-SVR responses exhibited changes in glycated hemoglobin (HbA1c), insulin, HOMA-IR, HOMA-beta, and plasma Tg levels

Next, the delayed responses in the control of plasma parameters after SVR were analyzed. When compared to the levels at baseline and at SVR (5.6 ± 0.1% vs. 5.8 ± 0.1%, p = 0.072), HbA1c level had a transient peak at pS6m (6.0 ± 0.1%; vs. baseline, p < 0.001 and vs. SVR, p = 0.001) but declined at pS1yr (vs. 5.8 + 0.1%, p = 0.016, Fig. 1C). Notably, the HbA1c value at pS6m was positively correlated with the plasma glucose level at SVR (r = 0.730, p < 0.001, Fig. 1D), which agreed with the concept that HbA1c can serve as an indicator of cumulative plasma glucose control in the preceding months. In addition, compared to the baseline, the post-SVR effects at pS6m and pS1yr involved a decline in insulin (10.0 ± 0.6 and 10.3 ± 0.6 vs. 14.9 ± 0.7 mIU/L, both p < 0.001, Fig. 1E), HOMA-IR (2.6 ± 0.2 and 2.8 ± 0.2 vs. 3.8 ± 0.2, p < 0.001 and p < 0.002, respectively, Fig. 1F), and HOMA-beta levels (104.7 ± 7.6 and 94.5 ± 5.2 vs. 154.5 ± 9.0, both p < 0.001, Fig. 1G) but increased plasma Tg levels (110.6 ± 5.5 and 114.4 ± 5.5 vs. 97.5.6 ± 3.4 mg/dL, p = 0.014 and p = 0.001, Fig. 1H).

Furthermore, further results revealed that the CHC patients may exhibit similar dynamic patterns from baseline

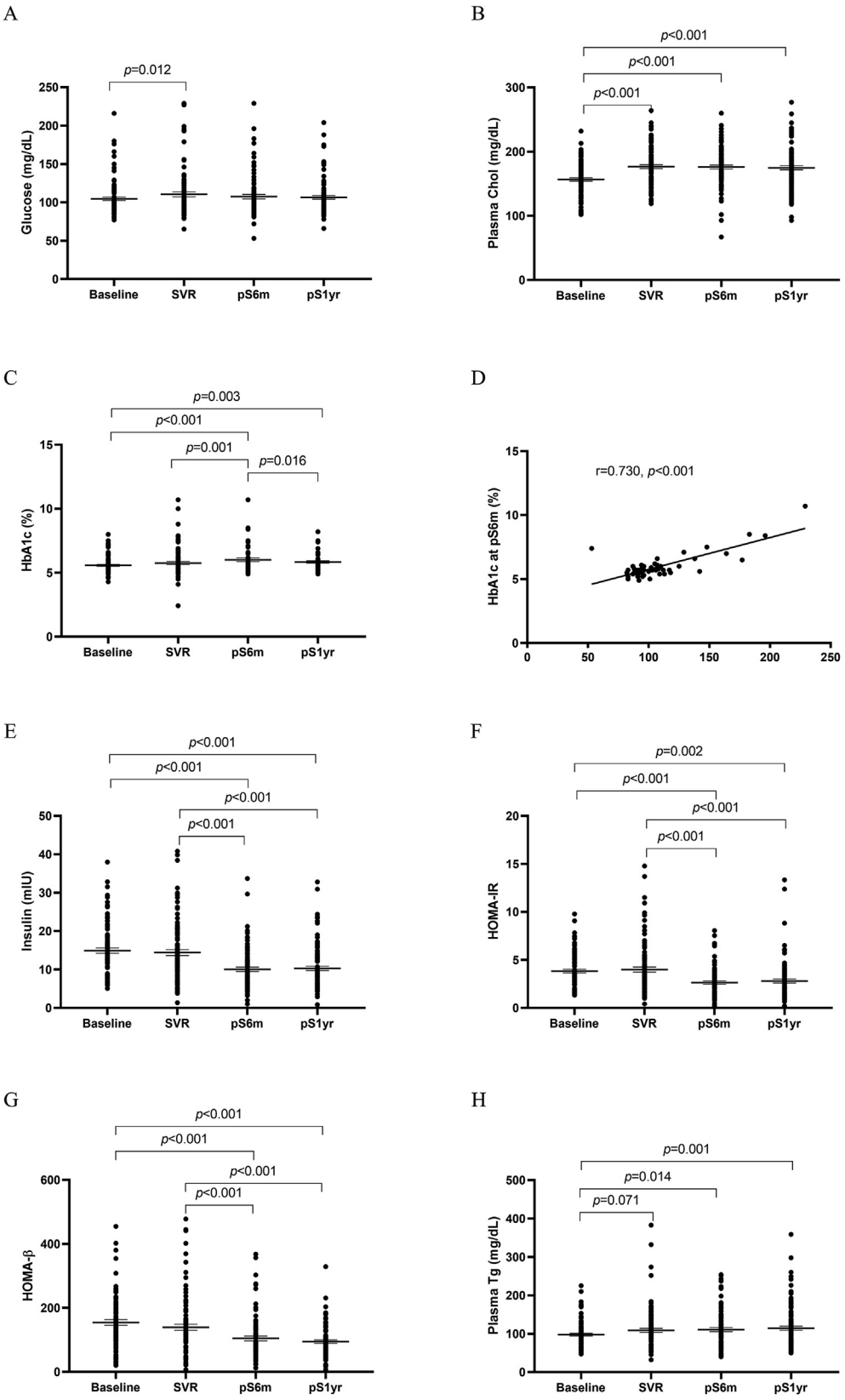

Figure 1. The profiles of plasma glycemic and lipid parameters. The levels of plasma (A) glucose, (B) Chol, (C) HbA1c, (E) insulin, and (H) Tg were determined at baseline, SVR, pS6m, and pS1yr in 95 CHC patients receiving DAA treatments. (D) The correlation between plasma glucose at SVR and HbA1c at pS6m. The scores of (F) HOMA-IR and (G) HOMA-beta were calculated and expressed at the indicated time points. The data were expressed as mean ± S.E.M. The statistical significance was evaluated via one-way ANOVA with repeated measures adjusted for age, gender, and HCV genotype in A, B, E, F, G, and H.

to pS1yr between HCV genotypes 1 and 2 for plasma Chol ($p = 0.969$), Tg ($p = 0.265$), glucose ($p = 0.983$), insulin ($p = 0.956$), HOMA-IR ($p = 0.696$), and HOMA-beta levels ($p = 0.861$) via the linear mixed model analysis adjusted for gender and age (Suppl. Fig. 1A—1F).

Lipoprotein lipid loads contributed to the posttherapeutic dynamics of plasma Chol and Tg

The plasma Chol (Fig. 2A, p values < 0.001) and Tg (Fig. 2B, p values < 0.01) levels were upregulated at posttherapy by ~15—20% from baseline. Next, the question was addressed as to whether the lipid loads in HDL and non-HDL may be modulated and which individual lipoprotein classes may account for the sustained increment of plasma Chol and Tg dynamics after DAA treatment. The results displayed the changes from baseline for plasma Chol and Tg levels, which demonstrated an inverse mirror in HDL, as the HDL-Chol level was upregulated by ~10% at SVR ($p = 0.001$) and returned to the baseline level at pS6m, whereas the HDL-Tg level exhibited a trend of downregulation from SVR to pS6m and returned at pS1yr (Fig. 2C). For the non-HDL lipoproteins, the results revealed upregulations of both Chol and Tg levels (Fig. 2D, p values < 0.01) from baseline to SVR, pS6m, and pS1yr.

Furthermore, the correlations of the lipid changes in plasma and in individual HDL, VLDL, and LDL samples within the three-time intervals of baseline-to-SVR, SVR-to-pS6m, and pS6m-to-pS1yr were examined. As a result, between baseline and SVR, the change in plasma Chol levels was positively correlated with HDL-Chol ($r = 0.552$, $p < 0.001$, Fig. 3A), but this change was not correlated with either VLDL-Chol or LDL-Chol loads (Table 1). Additionally, the change in plasma Tg levels was positively correlated with the change in LDL-Tg load ($r = 0.596$, $p < 0.001$, Fig. 3B), but this change was not correlated with either VLDL-Tg or HDL-Tg (Table 1). For the time interval from SVR to pS6m, the change of plasma Chol levels still exhibited a positive correlation with that of HDL-Chol ($r = 0.277$, $p = 0.010$, Fig. 3C), whereas neither correlations of changes occurred between plasma Chol with VLDL-Chol and LDL-Chol loads (Table 1). Additionally, correlations of changes between plasma Tg levels with HDL-Tg, VLLD-Tg, and LDL-Tg loads were not observed (Table 1). For the time interval between pS6m and pS1yr, the change of plasma Chol levels was not correlated with either changes in HDL, or in VLDL and LDL (Table 1), whereas the change of Tg levels in the plasma exhibited positive correlations with that in VLDL ($r = 0.406$, $p = 0.010$, Fig. 3D) and LDL ($r = 0.421$, $p = 0.008$, Fig. 3E), but not in HDL (Table 1).

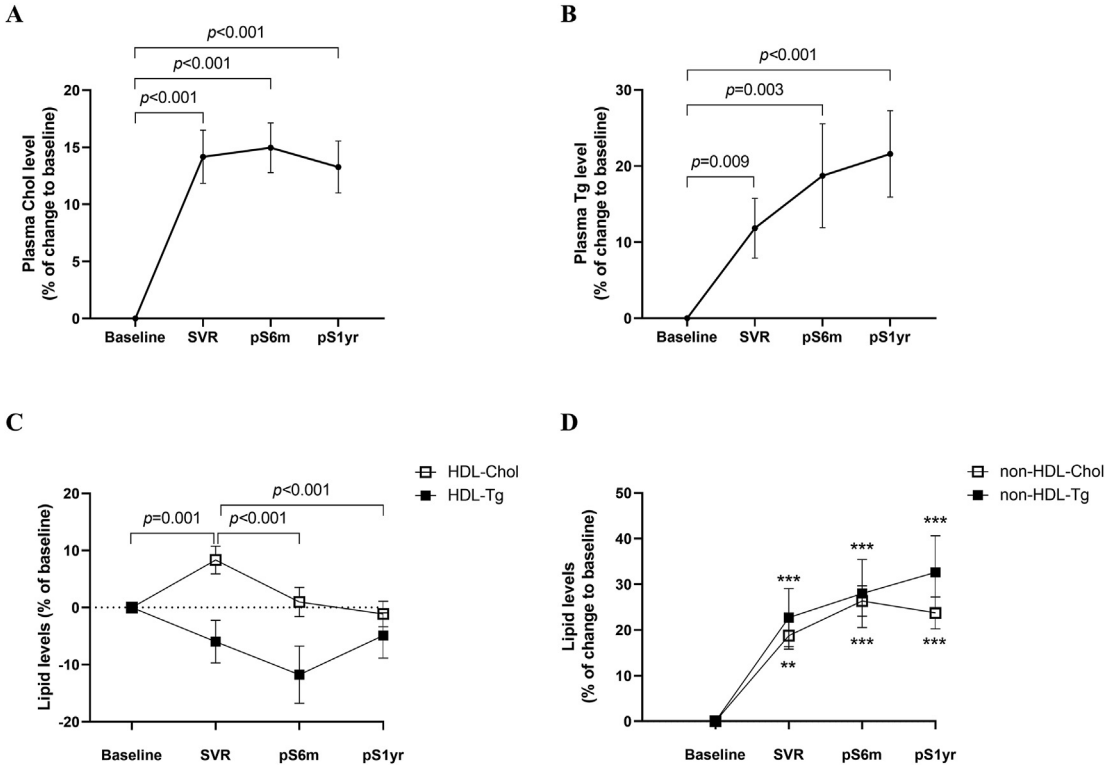

Figure 2. The dynamic changes in Chol and Tg in plasma, HDL, and non-HDL. The dynamic changes in (A) plasma Chol and (B) plasma Tg, as well as Chol and Tg, in (C) HDL and in (D) non-HDL at SVR, pS6m, and pS1yr were investigated. The results are presented as the percentage of changes to baseline and expressed as mean ± S.E.M. The statistical significance was evaluated via one-way ANOVA with repeated measures adjusted for age, gender, and HCV genotype. **, $p < 0.01$; and ***, $p < 0.001$ were indicated in D.

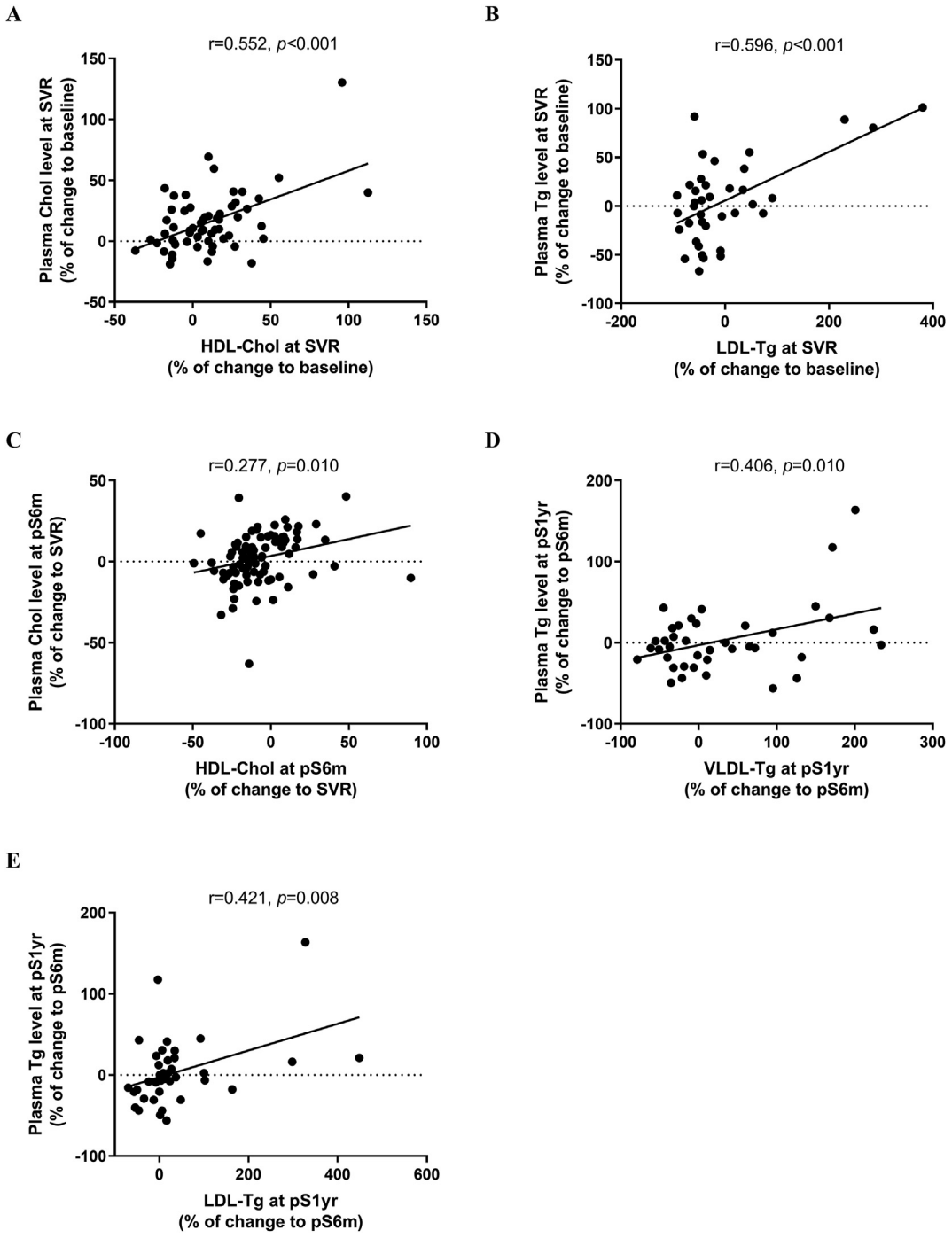

Figure 3. The correlations of the lipids between plasma and fractionated lipoproteins within intervals of baseline-to-SVR, SVR-to-pS6m, and pS6m-to-pS1yr. The correlations of the percentage changes between baseline and SVR for (A) plasma Chol and HDL-Chol, and for (B) plasma Tg and LDL-Tg; between SVR and pS6m for (C) plasma Chol and HDL-Chol; between pS6m and pS1yr for (D) plasma Tg and VLDL-Tg, and for (E) plasma Tg and LDL-Tg.

VLDL exhibited increased Tg and Chol loads *per* particle unit and underwent efficient Tg catabolism in the form of VLDL to LDL conversion

In comparison to the baseline, the VLDL-Tg was increasingly loaded *per* particle unit at SVR ($p = 0.006$), pS6m ($p = 0.016$), and pS1yr ($p = 0.048$) by ~50%; whereas the LDL-Tg load was unchanged at SVR, decreased at pS6m by ~50% ($p = 0.008$). Finally, and returned to the baseline levels at pS1yr (Fig. 4A). Furthermore, the *per* particle load of VLDL-Chol ($p = 0.010$) was elevated at SVR (Fig. 4B). Due to the fact that intravascular VLDL-to-LDL conversion may involve Tg hydrolysis and may decrease the LDL-Tg/VLDL-Tg ratio, the DAA effects on intravascular lipoprotein

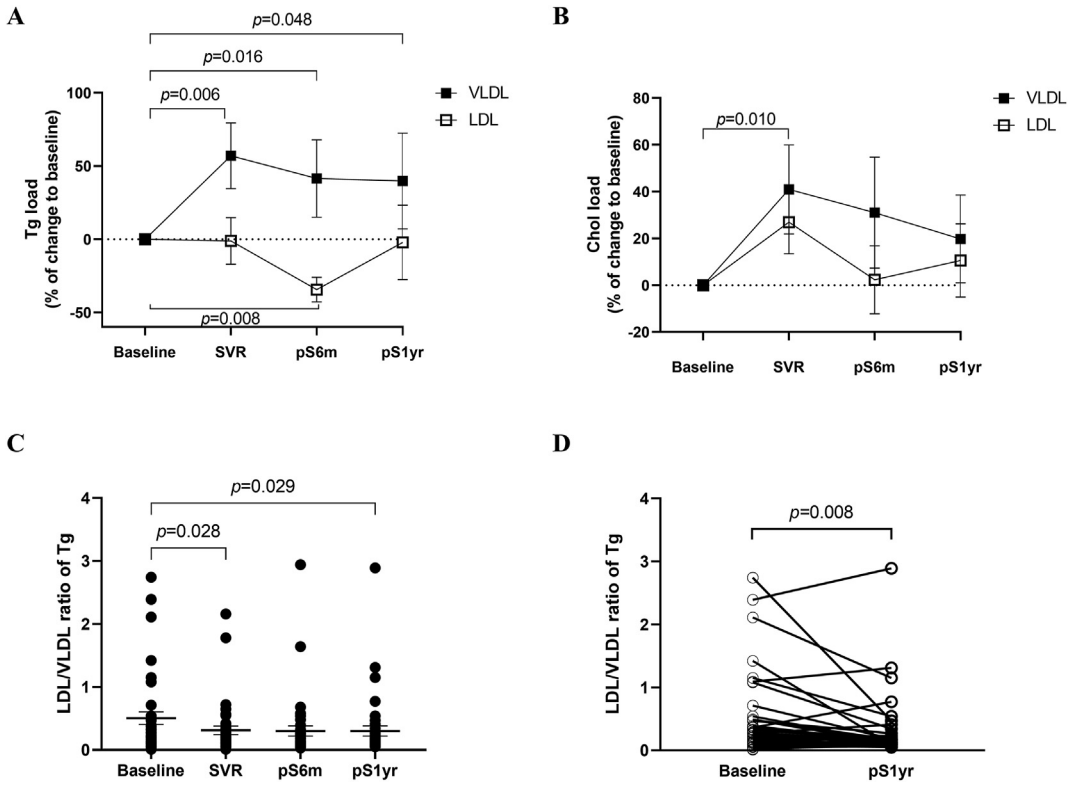

Figure 4. The dynamic changes in Chol and Tg loads in VLDL and LDL. The dynamic changes in (A) Tg and (B) Chol loads *per* VLDL and LDL particle unit at baseline, SVR, pS6m, and pS1yr were evaluated. The lipid loads were determined via the normalization of Tg and Chol levels with apoB and presented as the percentage of change to baseline. (C) The metabolic changes of Tg were evaluated by using the LDL/VLDL ratio. The results in A–C were expressed as mean ± S.E.M. and the statistical significance was evaluated via one-way ANOVA with repeated measures adjusted for age, gender, and HCV genotype. (D) Individual LDL/VLDL ratios of Tg at baseline and pS1yr were compared via the paired *t* test.

metabolism in patients were addressed via the analysis of the LDL/VLDL ratio of Tg. When compared to the baseline, the LDL/VLDL ratio of Tg was reduced at SVR (0.52 ± 0.10 *vs.* 0.31 ± 0.07, p = 0.028) and at pS1yr (*vs.* 0.30 ± 0.08, p = 0.029, Fig. 4C). Additionally, the reduction in the LDL/VLDL ratio of Tg between baseline and pS1yr in individual DAA-treated patients was further confirmed (Fig. 4D, p = 0.008).

Posttherapeutic dynamics exhibited interdependence between glycemic and lipid parameters

Next, the question was addressed as to whether the plasma glycemic and lipid parameters may exhibit dynamic interdependence. With the correlation being examined, the results revealed that the percentage of change from baseline to SVR for plasma glucose was positively correlated with that of plasma Chol (r = 0.451, p < 0.001, Fig. 5A) and HDL-Chol (r = 0.282, p = 0.006, Fig. 5B) but not with those of VLDL-Chol, LDL-Chol, plasma Tg, VLDL-Tg, LDL-Tg and HDL-Tg (Table 2). Subsequently, HDL-Chol was stratified by both upregulation and downregulation from baseline to SVR, thus showing comparable demographic and clinical backgrounds between the 2 groups at baseline (Suppl. Table 2). The further results showed changes in HDL-Chol from baseline to SVR exhibited positive correlations with HOMA-beta at pS6m (r = 0.371, p = 0.007, Fig. 5C) in the HDL-Chol upregulation group, but not in the downregulation group (r = 0.140, p = 0.470, Fig. 5D). As the subgroup of patients without diabetes was subsequently examined, the HDL-Chol upregulation group also exhibited a positive correlation between HOMA-beta at pS6m and the changes in HDL-Chol from baseline to SVR (r = 0.431, p = 0.004) but not the HDL-Chol downregulation group (r = 0.011, p = 0.966) (Suppl. Table 3 and Fig. 6A and B). Similarly, in the subgroup of CHC patients without metabolic syndrome, HOMA-beta at pS6m was correlated positively with the changes in HDL-Chol from baseline to SVR (r = 0.356, p = 0.039) but not in HDL-Chol downregulation group (r = 0.068, p = 0.762) (Suppl. Table 4 and Fig. 6C and D).

Discussion

Chronic HCV infection causes hepatic pathogenesis accompanied by multiple systemic metabolic complications; therefore, the therapeutic eradication of HCV may be promising in alleviating both liver damage and extrahepatic manifestations. The real-world results of DAA treatment in CHC patients have demonstrated higher efficiencies in reaching SVR and in alleviating liver disease

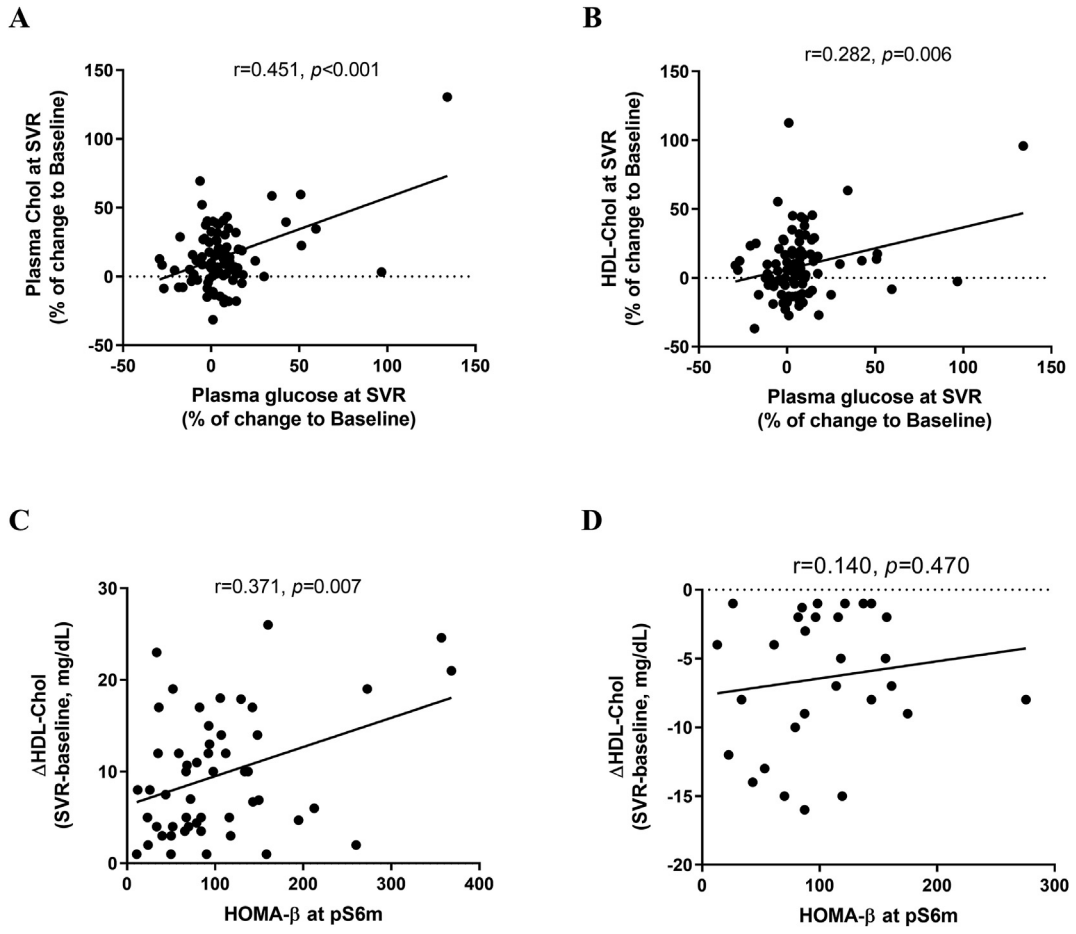

Figure 5. The correlations between glycemic and lipid parameters. The correlations of the percentage changes between baseline and SVR for (A) plasma glucose and plasma Chol, and for (B) plasma glucose and HDL-Chol; and the correlations of baseline-to-SVR HDL-Chol changes and HOMA-beta at pS6m in the CHC patient groups with (C) upregulation and (D) downregulation of HDL-Chol from baseline to SVR.

Table 2 The correlations between the changes of glycemic and lipid parameters from baseline to SVR (% of changes to baseline).

		Plasma glucose	HOMA-IR
Chol	Plasma	0.451 (<0.001)	0.298 (0.004)
	VLDL	0.194 (0.237)	0.210 (0.205)
	LDL	0.120 (0.417)	0.210 (0.211)
	HDL	0.282 (0.006)	0.174 (0.095)
Tg	Plasma	0.195 (0.060)	0.189 (0.069)
	VLDL	0.078 (0.637)	0.034 (0.939)
	LDL	0.277 (0.092)	0.627 (0.110)
	HDL	−0.068 (0.617)	−0.156 (0.251)

Data was expressed as Pearson coefficient (*p* value).

progression, as well as in producing better benefits in reducing cardiovascular events than the previous interferon-based regimens.[7] However, the direct or indirect mechanisms of these effects remain elusive and may contribute to the restoration of glycemic and lipid homeostasis after viremia clearance by using DAA treatment. In this study, the temporal and sequential regulations on blood parameters were analyzed to establish the interdependence of lipid and glycemic controls (Fig. 7).

With the plasma glycemic and lipid measurements, the surge of plasma glucose at SVR occurred earlier than the insulin response at pS6m (Fig. 1A and E), The results may indicate the existence of glucose regulation in an insulin-independent manner. Remarkably, the changes in plasma glucose and plasma Chol coincided at SVR, with a positive correlation in our results ($r = 0.451$, $p < 0.001$, Fig. 5A), as did plasma Chol with HDL-Chol ($r = 0.552$, $p < 0.001$, Fig. 3A) and HDL-Chol with plasma glucose ($r = 0.282$, $p = 0.006$, Fig. 5B), thus suggesting the regulatory interplay between plasma Chol, HDL-Chol, and plasma glucose. In addition to serving as canonical lipoprotein vesicles for reverse Chol transport, HDL can regulate glucose *via* plausible mechanisms involving direct enhancements of insulin-independent glucose uptake, insulin secretion from pancreatic beta cells, and insulin sensitivity.[25—27] Additionally, DAA treatment of CHC patients can induce the response of HDL-Chol elevation at SVR.[23,28—30] In this study, the simultaneous elevation of HDL-Chol at SVR (Fig. 2C) may be among the direct contributors providing insulin-

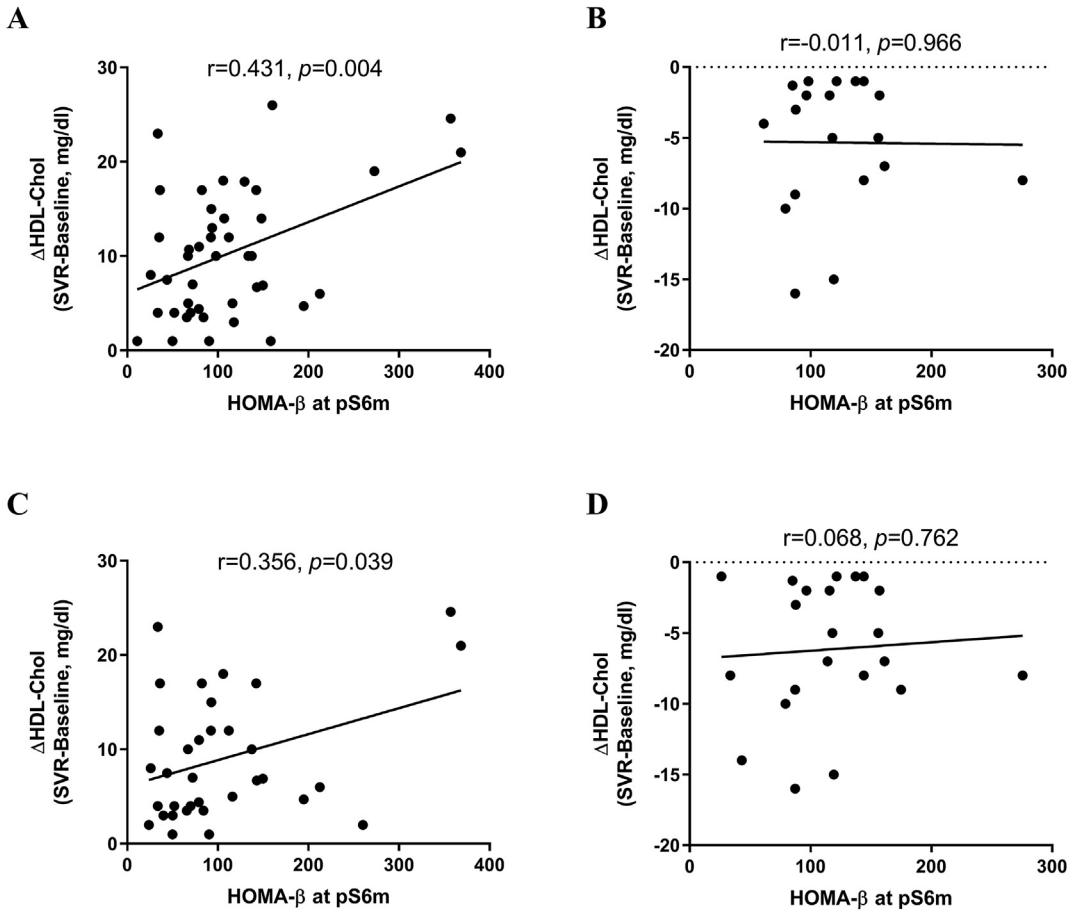

Figure 6. The posttherapeutic correlations of HDL-Chol and HOMA-beta in either nondiabetic or non-metabolic syndrome subgroups. The correlations of baseline-to-SVR HDL-Chol changes and HOMA-beta at pS6m in the nondiabetic subgroup of CHC patients with (A) upregulation and (B) downregulation of HDL-Chol from baseline to SVR; in the non-metabolic syndrome subgroup with (C) upregulation and (D) downregulation of HDL-Chol from baseline to SVR.

independent control of the transient SVR plasma glucose peak (Fig. 1A). Due to the fact that plasma glucose was used as a denominator in the HOMA-beta equation, it was reasonable to conclude that when the preceding increase in HDL-Chol led to a later decrease in plasma glucose, therefore, the baseline-to-SVR HDL-Chol changes may result in the positive correlation with HOMA-beta score at pS6m (Figs. 5C and 6A). Moreover, DAA treatment also improved insulin sensitivity post-SVR, as was evident by a steady decline in insulin and HOMA-IR levels from pS6m to pS1yr (Fig. 1E and F). Correspondingly, the sustained post-SVR decline in HOMA-beta scores (Fig. 1G), which might reset pancreatic beta-cell activities from compensation and dysfunction[31], may proceed as a function of the restoration of insulin sensitivity (Fig. 1E).

Chronic HCV infection can disturb lipid metabolism in many aspects, including the accumulation of excess fats in the liver by partially impairing lipoprotein assembly and egress from hepatocytes, thus predisposing CHC patients to hepatic steatosis and low circulating lipid levels, which can manifest with clinical signs such as hypocholesterolemia and hypobetalipoproteinemia. Accordingly, the release of viral effects with the DAA-treated eradication of HCV can alleviate hepatic lipid load, accompanied by the elevation of plasma Chol and non-HDL levels, however, which are generally considered to be a worsening of the blood lipid profile for CVD risk. In this study, DAA treatment increased VLDL-Tg and VLDL-Chol loads *per* secreted lipoprotein particle unit by 40—50% (Fig. 4A and B), which may constitute the underlying mechanism in favoring excess lipid export out of the liver, thus improving hepatic steatosis after the clearance of HCV infection. Moreover, the LDL/VLDL ratio Tg was shown to be decreased (Fig. 4C and D), which suggested that Tg hydrolysis may occur efficiently in the form of intravascular VLDL to LDL conversion. Furthermore, the positive correlations between the interval changes of plasma Chol and HDL-Chol (Fig. 3A and C) suggested that, again, the beneficial roles of HDL may counteract the CVD risks that induced by the pathogenic non-HDL lipoproteins, thus reconciling the discrepancy between the DAA-induced unfavorable plasma lipid profile, but reduced cardiovascular events in CHC patients with therapeutic SVR.

The heterogeneity of this study included HCV genotypes 1 and 2 and combined DAA regimens with and without ribavirin. Nevertheless, all of the CHC patients achieved SVR and were thereafter followed up for at least 1 year, which comprised a comprehensive analysis of the interplay

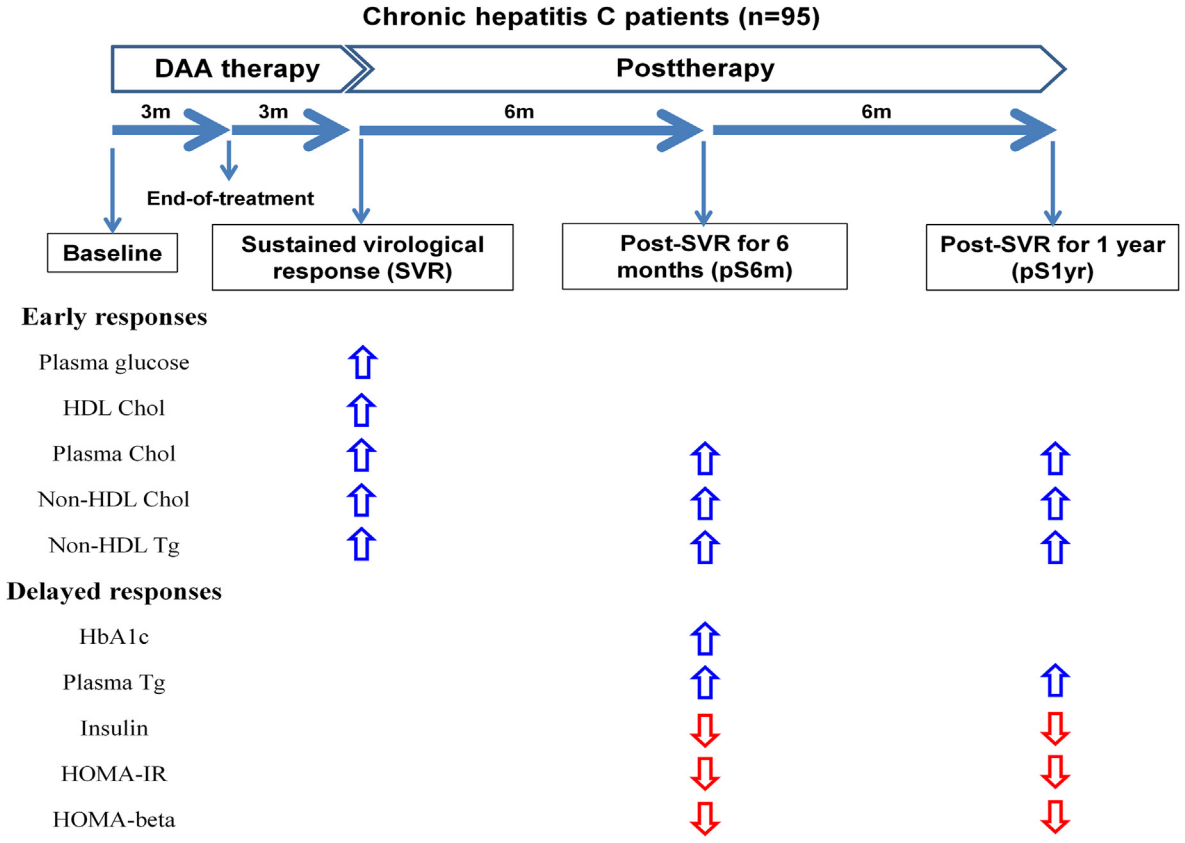

Figure 7. The Summary of temporal and sequential regulations on glycemic and lipid parameters of DAA posttherapy in chronic hepatitis C patients.

between blood glycemic and lipid phenotypical roles following HCV clearance.

This study initiated the evaluation on the post-therapeutic relationships of lipid and glycemic homeostatic modulation, with the novel finding showing interplay between plasma glycemic and lipid dynamics. In this study, the plasma lipid and glycemic parameters were analyzed to establish mutually modulatory relationships. The results showed coincidence of temporal and sequential regulations of each individual parameters (Figs. 1 and 7), as well as the positive correlations of dynamic changes (Figs. 5A—C, 6A, and 6C) between Chol, glucose, HDL, and HOMA-beta. Although many previous studies have showed the effects of DAA treatment of CHC patients which could restore metabolic functions, the current investigation added the merits of temporal, sequential, and interdependent regulations in plasma glycemic and lipid parameters. Our results provide evidence for the blood testing traits after successful DAA treatment and additionally may imply the impairment of HDL-Chol-glucose homeostatic network in CHC patients, which can be restored following clearance of HCV viremia.

In conclusion, irrespective of the baseline metabolic status, the posttherapeutic interdependence of glycemic and lipid modulation was revealed in CHC patients receiving DAA treatment.

Funding

The Ministry of Science and Technology of Taiwan, under the grants number MOST 108-2320-B-006-039-MY3 and 108-2314-B-006-089; National Cheng Kung University and Chi Mei Medical Center Joint Research Program, under the grant number CMNCKU10817; National Cheng Kung University and E-DA Hospital Joint Research Program, under the grant number NCKUEDA10803; NSFC grant, under the grant number 81971940.

Author Contribution

Contributors P-NC: Clinical sample collection, study concept and design, analysis and interpretation of data, drafting of the manuscript, obtaining funding; H-YS: Study concept and design, acquisition of data, analysis and interpretation of data, drafting of the manuscript; I-CF and Y-CC: Clinical sample collection; S-TW: analysis and interpretation of data, drafting of the manuscript; D-CT: Perform experiments, analysis and interpretation of data; H-CC and S-CC: Clinical sample collection; K-CY: Study concept and design, analysis and interpretation of data, drafting of the manuscript, critical revision of the manuscript for important intellectual content, obtaining funding, study supervision.

Declaration of competing interest

Pin-Nan Cheng, Hung-Yu Sun, I-Che Feng, Yen-Cheng Chiu, Sin-Tian Wang, Dyoness Charmaine Tan, Hung-Chih Chiu, Shih-Chih Chien, Kung-Chia Young have declared that they have no conflicts of interest to this study.

Acknowledgments

The authors would like to thank Ms. Li-Chi Chi and Jing-Ting Wu, and Mr. Yi-Hung Lee for their technical help and AJE English editing service.

References

1. Cacoub P, Comarmond C, Domont F, Savey L, Desbois AC, Saadoun D. Extrahepatic manifestations of chronic hepatitis C virus infection. *Ther Adv Infect Dis* 2016;**3**:3—14.
2. Spearman CW, Dusheiko GM, Hellard M, Sonderup M, Hepatitis C. *Lancet* 2019;**394**:1451—66.
3. Carrat F, Fontaine H, Dorival C, Simony M, Diallo A, Hezode C, et al. Clinical outcomes in patients with chronic hepatitis C after direct-acting antiviral treatment: a prospective cohort study. *Lancet* 2019;**393**:1453—64.
4. Younossi ZM, Stepanova M, Asselah T, Foster G, Patel K, Bräu N, et al. Hepatitis C in patients with minimal or No hepatic fibrosis: the impact of treatment and sustained virologic response on patient-reported outcomes. *Clin Infect Dis* 2018;**66**:1742—50.
5. Li J, Gordon SC, Rupp LB, Zhang T, Trudeau S, Holmberg SD, et al. Sustained virological response to hepatitis C treatment decreases the incidence of complications associated with type 2 diabetes. *Aliment Pharmacol Ther* 2019;**49**:599—608.
6. McGlynn EA, Adams JL, Kramer J, Sahota AK, Silverberg MJ, Shenkman E, et al. Assessing the safety of direct-acting antiviral agents for hepatitis C. *JAMA Netw Open* 2019;**2**:e194765.
7. Butt AA, Yan P, Shuaib A, Abou-Samra AB, Shaikh OS, Freiberg MS. Direct-acting antiviral therapy for HCV infection is associated with a reduced risk of cardiovascular disease events. *Gastroenterology* 2019;**156**:987—96. e988.
8. Adinolfi LE, Petta S, Fracanzani AL, Coppola C, Narciso V, Nevola R, et al. Impact of hepatitis C virus clearance by direct-acting antiviral treatment on the incidence of major cardiovascular events: a prospective multicentre study. *Atherosclerosis* 2020;**296**:40—7.
9. Bose SK, Ray R. Hepatitis C virus infection and insulin resistance. *World J Diabetes* 2014;**5**:52—8.
10. Kawaguchi T, Yoshida T, Harada M, Hisamoto T, Nagao Y, Ide T, et al. Hepatitis C virus down-regulates insulin receptor substrates 1 and 2 through up-regulation of suppressor of cytokine signaling 3. *Am J Pathol* 2004;**165**:1499—508.
11. Banerjee S, Saito K, Ait-Goughoulte M, Meyer K, Ray RB, Ray R. Hepatitis C virus core protein upregulates serine phosphorylation of insulin receptor substrate-1 and impairs the downstream akt/protein kinase B signaling pathway for insulin resistance. *J Virol* 2008;**82**:2606—12.
12. Sheikh MY, Choi J, Qadri I, Friedman JE, Sanyal AJ. Hepatitis C virus infection: molecular pathways to metabolic syndrome. *Hepatology* 2008;**47**:2127—33.
13. Kasai D, Adachi T, Deng L, Nagano-Fujii M, Sada K, Ikeda M, et al. HCV replication suppresses cellular glucose uptake through down-regulation of cell surface expression of glucose transporters. *J Hepatol* 2009;**50**:883—94.
14. Shoji I, Deng L, Hotta H. Molecular mechanism of hepatitis C virus-induced glucose metabolic disorders. *Front Microbiol* 2011;**2**:278.
15. Grassi G, Di Caprio G, Fimia GM, Ippolito G, Tripodi M, Alonzi T. Hepatitis C virus relies on lipoproteins for its life cycle. *World J Gastroenterol* 2016;**22**:1953—65.
16. Vieyres G, Pietschmann T. *Tracking hepatitis C virus interactions with the hepatic lipid metabolism*. The Liver; 2020. p. 889—905.
17. Miyanari Y, Atsuzawa K, Usuda N, Watashi K, Hishiki T, Zayas M, et al. The lipid droplet is an important organelle for hepatitis C virus production. *Nat Cell Biol* 2007;**9**:1089—97.
18. Merz A, Long G, Hiet MS, Brügger B, Chlanda P, Andre P, et al. Biochemical and morphological properties of hepatitis C virus particles and determination of their lipidome. *J Biol Chem* 2011;**286**:3018—32.
19. Lowey B, Hertz L, Chiu S, Valdez K, Li Q, Liang TJ. Hepatitis C virus infection induces hepatic expression of NF-κB-Inducing kinase and lipogenesis by downregulating miR-122. *mBio* 2019;**10**:e01617—9.
20. Amako Y, Munakata T, Kohara M, Siddiqui A, Peers C, Harris M. Hepatitis C virus attenuates mitochondrial lipid β-oxidation by downregulating mitochondrial trifunctional-protein expression. *J Virol* 2015;**89**:4092—101.
21. Chaudhari R, Fouda S, Sainu A, Pappachan JM. Metabolic complications of hepatitis C virus infection. *World J Gastroenterol* 2021;**27**:1267—82.
22. Lim T. Metabolic syndrome in chronic hepatitis C infection: does it still matter in the era of directly acting antiviral therapy? *Hepat Med* 2014;**6**:113—8.
23. Sun HY, Cheng PN, Tseng CY, Tsai WJ, Chiu YC, Young KC. Favouring modulation of circulating lipoproteins and lipid loading capacity by direct antiviral agents grazoprevir/elbasvir or ledipasvir/sofosbuvir treatment against chronic HCV infection. *Gut* 2018;**67**:1342—50.
24. Song Y, Manson JE, Tinker L, Howard BV, Kuller LH, Nathan L, et al. Insulin sensitivity and insulin secretion determined by homeostasis model assessment and risk of diabetes in a multiethnic cohort of women: the Women's Health Initiative Observational Study. *Diabetes Care* 2007;**30**:1747—52.
25. Drew BG, Rye KA, Duffy SJ, Barter P, Kingwell BA. The emerging role of HDL in glucose metabolism. *Nat Rev Endocrinol* 2012;**8**:237—45.
26. Siebel AL, Heywood SE, Kingwell BA. HDL and glucose metabolism: current evidence and therapeutic potential. *Front Pharmacol* 2015;**6**:258.
27. Waldman B, Jenkins AJ, Sullivan D, Ng MKC, Keech AC. HDL as a target for glycemic control. *Curr Drug Targets* 2017;**18**:651—73.
28. Graf C, Welzel T, Bogdanou D, Vermehren J, Beckel A, Bojunga J, et al. Hepatitis C clearance by direct-acting antivirals impacts glucose and lipid homeostasis. *J Clin Med* 2020;**9**:2702.
29. Shimizu K, Soroida Y, Sato M, Hikita H, Kobayashi T, Endo M, et al. Eradication of hepatitis C virus is associated with the attenuation of steatosis as evaluated using a controlled attenuation parameter. *Sci Rep* 2018;**8**:7845.
30. Endo D, Satoh K, Shimada N, Hokari A, Aizawa Y. Impact of interferon-free antivirus therapy on lipid profiles in patients with chronic hepatitis C genotype 1b. *World J Gastroenterol* 2017;**23**:2355—64.
31. Hudish LI, Reusch JE, Sussel L. β Cell dysfunction during progression of metabolic syndrome to type 2 diabetes. *J Clin Invest* 2019;**129**:4001—8.

Appendix A. Supplementary data

Supplementary data to this article can be found online at https://doi.org/10.1016/j.jmii.2022.06.004.